

# Journal of Materials Chemistry A

Accepted Manuscript



This is an *Accepted Manuscript*, which has been through the Royal Society of Chemistry peer review process and has been accepted for publication.

*Accepted Manuscripts* are published online shortly after acceptance, before technical editing, formatting and proof reading. Using this free service, authors can make their results available to the community, in citable form, before we publish the edited article. We will replace this *Accepted Manuscript* with the edited and formatted *Advance Article* as soon as it is available.

You can find more information about *Accepted Manuscripts* in the [Information for Authors](#).

Please note that technical editing may introduce minor changes to the text and/or graphics, which may alter content. The journal's standard [Terms & Conditions](#) and the [Ethical guidelines](#) still apply. In no event shall the Royal Society of Chemistry be held responsible for any errors or omissions in this *Accepted Manuscript* or any consequences arising from the use of any information it contains.

Cite this: DOI: 10.1039/c0xx00000x

www.rsc.org/xxxxxx

## COMMUNICATION

**Facile Preparation of Ultrathin Sulfur-Wrapped Polyaniline Nanofiber Composite with Core-Shell structure as High Performance Cathode Material of Lithium-Sulfur Battery**Hong Gao,<sup>a,b</sup> Qi Lu,<sup>a</sup> Nianjiang Liu,<sup>a</sup> Xianhong Wang<sup>\*a</sup> and Fosong Wang<sup>a</sup><sup>5</sup> Received (in XXX, XXX) XthXXXXXXXXXX 20XX, Accepted Xth XXXXXXXXXXXX 20XX

DOI: 10.1039/b000000x

**Ultrathin sulfur layer (10nm) wrapped polyaniline (PANI) nanofiber composite (S-PANI) with core-shell structure was prepared via facile heterogeneous nucleation of sulfur on water dispersed PANI nanofiber, which displayed initial discharge capacity of 977 mAh g<sup>-1</sup> and 88.3% of capacity retention after 100 cycles at 1 C.**

Lithium-sulfur (Li-S) battery is showing great possibility as a promising successor for the next generation high-energy-density battery. One reason is that it has a theoretical specific energy of *Ca.* 2600 Wh kg<sup>-1</sup>, which is more than 5 times that of conventional lithium ion battery, as calculated from the electrochemical reaction  $16 \text{ Li} + \text{S}_8 \rightarrow 8 \text{ Li}_2\text{S}$ , and another advantage lies in that sulfur is inexpensive and abundant on the earth, well suitable for large-scale practical application.<sup>1</sup> Nevertheless, the practical application of Li-S battery has not yet been achieved because of some challenges like low practical capacity and poor cycle performance, especially at high charge/discharge rate, mainly due to the insulating feature of sulfur, significant structure and volumetric change during the cycling process, and the “shuttle” phenomenon caused by the high solubility of intermediate reduction products  $\text{Li}_2\text{S}_x$  ( $2 < x \leq 8$ ) in organic electrolytes.<sup>2-4</sup>

In recent years, much effort has been made to fabricate high performance Li-S battery. The electronic conductivity and structural stability of the cathode were enhanced by combining sulfur with conducting matrix, commonly carbon materials like microporous carbon,<sup>5</sup> mesoporous carbon,<sup>6-7</sup> engineered hierarchical porous carbon,<sup>8</sup> hollow carbon sphere,<sup>9</sup> carbon nanotube,<sup>10</sup> carbon nanofiber<sup>11</sup> and grapheme.<sup>12-14</sup> Recently, Chen and co-workers designed a layered porous carbon-sulfur composite consisting of a graphene layer with thin layers of porous carbon uniformly covering both surfaces, which showed a very high initial discharge capacity of 885 mAh g<sup>-1</sup> at 0.5 C and 70% capacity retention after running 100 cycles.<sup>15</sup> Nazar and coworkers confined sulfur in 4-5 nm mesopores in the shell and inner lining of the carbon nanospheres, a specific capacity of over 875 mAh g<sup>-1</sup> was achieved at 1 C with a fade rate of 0.1% per cycle.<sup>16</sup> The sulfur in these materials was in nano-scale, which not

only improved its utilization but also increased the contact area with conducting matrixes. And just like these, confining sulfur in the pores of various carbon materials has been a usual strategy to prevent the loss of soluble polysulfides. However, the physical encapsulating method is not as perfect as expected, further research by Cui's group showed that the insoluble  $\text{Li}_2\text{S}/\text{Li}_2\text{S}_2$  would detach from the carbon surface during discharge due to the low binding energy between the nonpolar carbon and polar  $\text{Li}_2\text{S}/\text{Li}_2\text{S}_2$  clusters, resulting in loss of electrical contact and capacity decay.<sup>17</sup> Therefore, to effectively hold sulfur within the conducting materials, attention should be focused on designing more reasonable structure or developing alternative matrix to carbon.

Inspired by above reports, we tried to search a positively-charged conducting matrix replacing carbon materials to combine with sulfur in nano-scale. Compared with the single physical adsorption of carbon materials, the electrostatic interaction of positively-charged conducting matrix to negatively-charged  $\text{S}_x^{2-}$  ( $2 < x \leq 8$ ) could be stronger during the charge/discharge process. Conducting polymers may meet the need by positively charging the backbones through acid doping. In fact, previous reports proved that they surely owned the abilities to absorb and hold sulfur.<sup>18-25</sup> Here, we chose polyaniline (PANI) nanofibers with requisite positively-charged backbones as the matrix material. Compared with S-PANI composite previously reported, PANI nanofibers used here were thinner (with an average diameter of 70 nm) and water dispersed which ensured that organic solvent was non-essential and all producing processes could be carried out in water. Beyond that, no thermal treatment applied from beginning to end, so conducting matrix kept their original structure and conductivity. To insure the efficient ion transmission and electron conveying at different discharge rate, the sulfur was deposited on the outer surface of PANI nanofiber. The thickness of this sulfur layer was determined as 10 nm, nearly equalling the maximum thickness of typical electric double layer on the surface of electrode.<sup>26</sup> That could, for one thing, maximize the utilization of electrostatic interaction, and for another, increase the sulfur content in this composite as high as possible. The sulfur content in this designed

composite could be calculated by the following equation:

$$S\% = W_s / (W_s + W_{PANI}) \quad \text{eq.1}$$

The eq.1 could be further derived as eq.2 (more detailed discussion see Supporting Information):

$$t_s = r \left\{ \left[ \frac{S\%}{1 - S\%} + \frac{\gamma \rho_s}{\rho_{PANI}} \frac{\rho_{PANI}}{\gamma \rho_s} \right]^{1/2} - 1 \right\} \quad \text{eq.2}$$

where  $S\%$  is the sulfur content in the composite,  $W_s$  is the mass of sulfur,  $W_{PANI}$  is the mass of PANI,  $\gamma$  is the correction factor (approximately equals to 1.0),  $\rho_s$  is the sulfur density ( $1.96 \text{ g cm}^{-3}$ ),  $\rho_{PANI}$  is the PANI density ( $0.75 \text{ g cm}^{-3}$ ),  $r$  is the PANI radius (35 nm), and  $t_s$  is the thickness of the sulfur layer (10 nm). It was easily concluded that the sulfur content in this composite was no less than 60%, a relatively high value for the sulfur electrode material. By adjusting experiment conditions, finally we successfully prepared this ultrathin sulfur-wrapped PANI nanofiber for the first time.

Referring to the former work of our group, the water dispersed conducting PANI nanofibers with diameter of about 70 nm were synthesized in large quantity and used as template to prepare the sulfur-wrapped PANI composite by the heterogeneous nucleation reaction.<sup>27-28</sup> Zeta potential of the PANI was about +45.17 mV, so thiosulfate ions could be adsorbed around the positively-charged PANI nanofibers easily during the nucleation reaction. Next, elemental sulfur nucleated on the dispersed PANI substrates after dropping sulphuric acid solution into the mixture. All the reactions were carried out in water at ambient atmosphere without heating, the facile synthesis process made it suitable for large-scale preparation. PANI nanofibers used here showed a high BET specific surface area of  $77.14 \text{ m}^2 \text{ g}^{-1}$  and a total pore volume of  $0.24 \text{ cm}^3 \text{ g}^{-1}$ , which was very important for effective sulfur deposition. After deposition process, the sulfur can fill the void of PANI nanofibers, since the BET surface area and pore volume of S-PANI dropped to  $24.33 \text{ m}^2 \text{ g}^{-1}$  and  $0.12 \text{ cm}^3 \text{ g}^{-1}$ , respectively. (Fig. 1a)

The sulfur loading in the S-PANI composite was determined by thermogravimetric analysis (TGA). As shown in Fig. 1b, the elemental sulfur started a weight loss at  $120^\circ\text{C}$  and lost its all weight at  $300^\circ\text{C}$ , while the PANI exhibited little weight loss (12.18%) within this range of temperature, mainly due to the loss of moisture and decomposition of PANI itself. As for S-PANI composites, considered the low content of PANI in this composite, weight loss of inner PANI could be ignored when sulfur was evaporating, and it was easy to conclude that the sulfur loading was about 65%.

Fig. 1c shows the X-ray diffraction (XRD) patterns of elemental sulfur, PANI nanofiber and S-PANI composite, respectively. Two prominent peaks at  $2\theta = 23$  and  $28^\circ$  corresponding to an  $F_{dd}$  orthorhombic structure can be observed in XRD pattern of elemental sulfur. While XRD pattern of PANI nanofiber shows two broad, low-intensity peaks centered at  $2\theta = 19.1$  and  $25.4^\circ$ , which could be assigned as the periodicity parallel and perpendicular to the PANI chains, respectively. The diffraction peaks of elemental sulfur are visible in XRD pattern of the S-PANI composite, though the intensities become distinctly lower, it still indicated that the sulfur formed by heterogeneous nucleation retained its original crystal structure.

X-ray photoelectron spectroscopy (XPS) was used to study the

sulfur wrapping on the PANI. Fig. 1d shows S 2p spectra of S-PANI and sulfur produced by mixing sodium thiosulfate with sulfuric acid. Two types of S atoms in S-PANI were observed with the binding energies of 167.15 and 163.35 eV. One at 163.35 eV came from the dopant  $\text{SO}_4^{2-}$ , which replaced the initial dopant phosphate ester during acid titrating process, and the other at 167.15 eV matched well with the characteristic peak of sulfur implying that sulfur had deposited on the polyaniline nanofiber successfully.

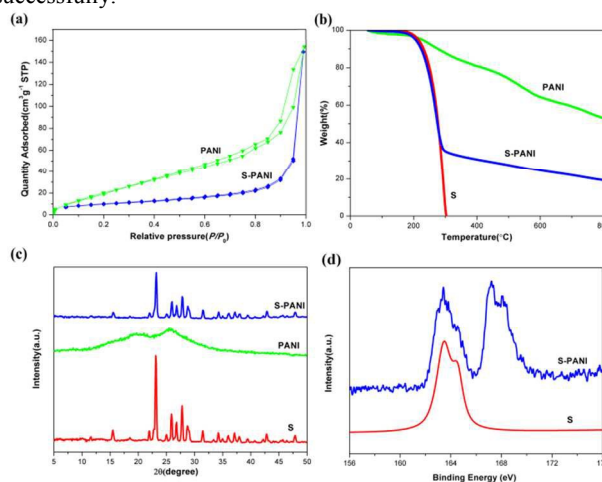


**Fig. 1** (a) Nitrogen adsorption-desorption isotherms of PANI and S-PANI; (b) TGA curves of S, PANI, and S-PANI; (c) XRD patterns of S, PANI, and S-PANI; (d) XPS spectra of S 2p for S and S-PANI.

The morphology characterizations of S-PANI composite were carefully investigated by scanning electron microscopy (SEM) and transmission electron microscopy (TEM). Fig. 2a shows the SEM image of S-PANI composite. It displayed neat wire-like shape. The SEM elemental mapping images (Fig. 2b) displayed matching spatial distributions of C, N and S, indicating the uniform distribution of sulfur in the S-PANI composite. EDX microanalysis (lower right image in Fig. 2b) exhibited a strong sulfur signal, which was higher than carbon. The existence of oxygen was from the dopant  $\text{SO}_4^{2-}$ . TEM was used to further study the core-shell structure and track the elemental distribution of carbon, nitrogen and sulfur in the S-PANI composite. The S-PANI composite was fiber-like with diameter of about 90 nm, and the thickness of sulfur wrapped on PANI nanofiber was just *ca.* 10 nm. However, the boundary between sulfur and PANI was very clear even under such thin sulfur coverage. As shown in Fig. 2d, the sulfur can keep uniform distribution on single PANI nanofiber.

The above morphology characterizations confirmed that the ultrathin sulfur-wrapped polyaniline nanofiber composite was successfully synthesized. This well-designed structure was beneficial for electrochemical performance. Inner conductive PANI nanofibers formed an effective and stable electron transport system, like carbon material. During charge/discharge progress, the positively-charged backbone could hold negatively-charged  $\text{S}_x^{2-}$  ( $2 < x \leq 8$ ) by the electrostatic interaction, which assured its cycle stability. While the outer extremely thin layer of sulfur made the diffusion of ions between cathode and electrolyte easier and faster, showing the potential of high utilization of active

materials and good electrochemical performance in high discharge rate. The electrochemical performances of S-PANI composite cathodes were examined in CR2016-type coin cells, which were fabricated by sandwiching a porous polypropylene separator (Celgard 2500) between the S-PANI electrode and Li foil, the electrolyte was 1.0 M lithium bis(trifluoromethane) sulfonamide (LiTFSI) in a mixed solvent of 1,3-dioxolane (DOL) and 1,2-dimethoxyethane (DME) (1:1, v/v).

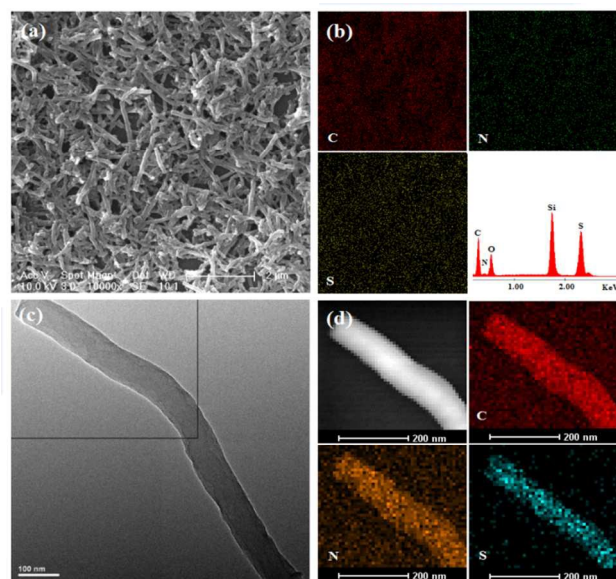


**Fig. 2** Morphology of S-PANI composite: (a) SEM image; (b) SEM elemental maps of carbon (upper left), nitrogen (upper right), sulfur (lower left), and the EDX pattern (lower right); (c) TEM image; (d) Dark-field TEM (upper left), and EDX elemental mappings of carbon (upper right), nitrogen (lower left) and sulfur (lower right).

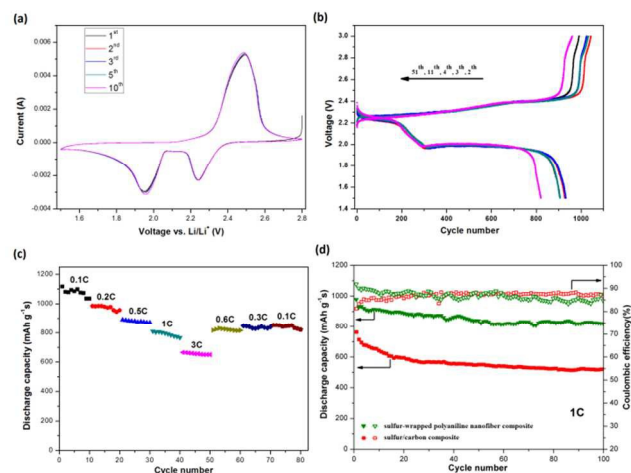
Fig. 3a shows the cyclic voltammogram (CV) curves of S-PANI nano-composite. During the first reduction process, two main reduction peaks appeared at around 2.24 V and 1.95 V, characteristic of the two-step reduction of elemental sulfur, the first step was the transformation from cyclo-octasulfur ( $S_8$ ) to long-chain soluble lithium polysulfides ( $Li_2S_x$ ,  $4 \leq x < 8$ ), while the second step corresponded to the decomposition of polysulfides to form insoluble short-chain lithium sulfides ( $Li_2S_2$  and/or  $Li_2S$ ). In the subsequent anodic scan, oxidation peak was found at around 2.49 V, which corresponded to the conversion of  $Li_2S$  into high-order soluble polysulfides.<sup>25</sup> The cyclic voltammograms showed no obvious change in the following scans up to 10 cycles, indicating excellent reversibility and cycling stability of S-PANI composite.

Fig. 3b shows the galvanostatic charge-discharge profiles of S-PANI electrode at 1 C during different cycles. There are two apparent discharge plateaus and one charge plateau on each curve, which matches well with the CV measurements. The decrease of specific capacity was insignificant with the increasing cycle number, e.g., the fourth cycle and eleventh cycle were even superposition.

Fig. 3c shows the rate capacity performance of the S-PANI composite electrode. After an initial discharge capacity of 1116

mAh  $g^{-1}$  at 0.1 C, the capacity was found to stabilize around 1080 mAh  $g^{-1}$ , and it was 980 mAh  $g^{-1}$  at 0.2 C. Further cycling at 0.5, 1 and 3 C, it still showed high reversible capacities of 890, 808 and 655 mAh  $g^{-1}$ , respectively. When the current density was switched from 3 to 0.6 C, the specific capacity was largely recovered at the 51th cycle, indicating good reversible stability of this cathode material.

This composite cathode showed superior electrochemical performance producing a high initial discharge capacity of 977 mAh  $g^{-1}$  at 1 C. Since the second cycle, the specific capacity stabilized at high capacities of approximate 900 mAh  $g^{-1}$  and 88.3% of the initial capacity was retained after 100 cycles (Fig. 3d). As a reference, the sulfur/carbon composite was prepared by ball-milling and 180 °C thermal treatment, an initial discharge capacity of 762 mAh  $g^{-1}$  was obtained, and it dropped to 520 mAh  $g^{-1}$  after 100 cycles. This comparison clearly showed that the core-shell structure of sulfur-wrapped PANI composite could offer more advantages to improve the electrochemical performance of the Li-S battery than traditional sulfur/carbon material.



**Fig. 3** (a) Cyclic voltammograms of S-PANI composite; (b) Discharge-charge voltage profiles of S-PANI composite at 1 C; (c) Rate performance of S-PANI composite at various cycling rate from 0.1 to 3 C with respect to cycle number; (d) Cycle stability of the S-PANI composite and S-C composite at 1 C.

In summary, an ultrathin sulfur-wrapped PANI nano-composite was well-designed and successfully prepared by a very simple and soft route. This novel S-PANI composite exhibited a high initial discharge capacity of 977 mAh  $g^{-1}$  and 88.3% of capacity retention after 100 cycles at 1 C, which represents the best comprehensive performance among the PANI composite used in Li-S batteries so far. The high specific capacity and good cycle stability at high rate demonstrated the rationality of this special three-dimensional structure. Conducting PANI nanofiber with positively-charged backbone not only acted like stable carbon materials transmitting electrons but also could hold negatively-charged  $S_x^{2-}$  ( $2 < x < 8$ ) around it during the charge/discharge process. In addition, the ultrathin sulfur of outer layer made ion transmission more fast and convenient, meanwhile, the utilization of active material was largely improved compared with the traditional S-C material.

The authors thank financial support from the Natural Science

Foundation of China (Grant Nos. 51321062 and 51303168).

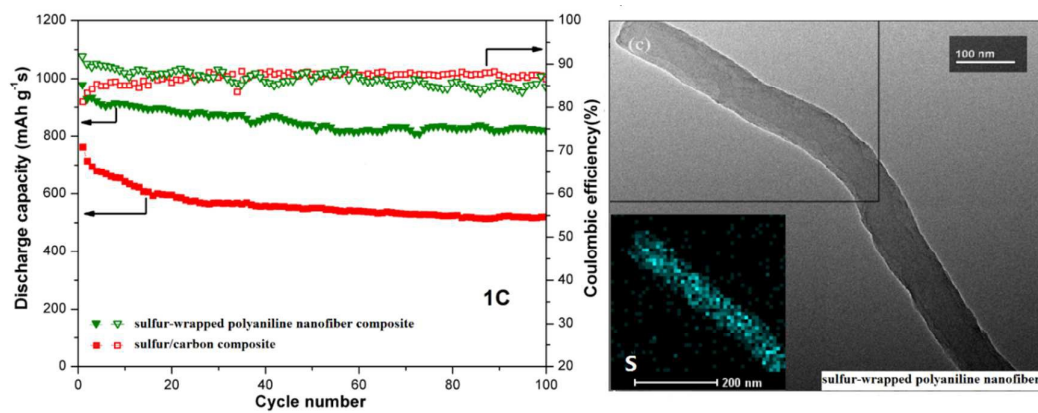
## Notes and references

<sup>a</sup>Key Laboratory of Polymer Eco-materials, Changchun Institute of Applied Chemistry, Chinese Academy of Sciences, Changchun 130022, People's Republic of China. Fax: 86431 85689095; Tel: 86431 85262250; E-mail: xhwang@ciac.jl.cn

<sup>b</sup>University of Chinese Academy of Sciences, Beijing 100039, People's Republic of China.

† Electronic Supplementary Information (ESI) available: Experimental details and additional data. See DOI: 10.1039/b000000x/

- 1 D. Bresser, S. Passerini and B. Scrosati, *Chem. Commun.*, 2013, **49**, 10545–10562.
- 2 A. Manthiram, Y. Fu and Y. S. Su, *Acc. Chem. Res.*, 2013, **46**, 1125–1134.
- 3 M. K. Song, E. J. Cairns and Y. Zhang, *Nanoscale*, 2013, **5**, 2186–2204.
- 4 L. Chen and L. L. Shaw, *J. Power Sources*, 2014, **267**, 770–783.
- 5 S. Xin, L. Gu, N. H. Zhao, Y. X. Yin, L. J. Zhou, Y. G. Guo and L. J. Wan, *J. Am. Chem. Soc.*, 2012, **134**, 18510–18513.
- 6 X. Ji, K. T. Lee and L. F. Nazar, *Nat. Mater.*, 2009, **8**, 500–506.
- 7 J. Schuster, G. He, B. Mandlmeier, T. Yim, K. T. Lee, T. Bein and L. F. Nazar, *Angew. Chem., Int. Ed.*, 2012, **51**, 3591–3595.
- 8 B. Ding, C. Yuan, L. Shen, G. Xu, P. Nie and X. Zhang, *Chem. Eur. J.*, 2013, **19**, 1013–1019.
- 9 N. Jayaprakash, J. Shen, S. S. Moganty, A. Corona and L. A. Archer, *Angew. Chem., Int. Ed.*, 2011, **50**, 5904–5908.
- 10 J. Guo, Y. Xu and C. Wang, *Nano Lett.*, 2011, **11**, 4288–4294.
- 11 G. Zheng, Y. Yang, J. J. Cha, S. S. Hong and Y. Cui, *Nano Lett.*, 2011, **11**, 4462–4467.
- 12 K. Xi, P. R. Kidambi, R. Chen, C. Gao, X. Peng, C. Ducati, S. Hofmann and R. V. Kumar, *Nanoscale*, 2014, **6**, 5746–5753.
- 13 J. Zhang, Z. Dong, X. Wang, X. Zhao, J. Tu, Q. Su and G. Du, *J. Power Sources*, 2014, **270**, 1–8.
- 14 H. Kim, H. D. Lim, J. Kim and K. Kang, *J. Mater. Chem. A*, 2014, **2**, 33–47.
- 15 X. Yang, L. Zhang, F. Zhang, Y. Huang and Y. Chen, *ACS Nano*, 2014, **8**, 5208–5215.
- 16 G. He, S. Evers, X. Liang, M. Cuisinier, A. Garsuch and L. F. Nazar, *ACS Nano*, 2013, **7**, 10920–10930.
- 17 G. Zheng, Q. Zhang, J. J. Cha, Y. Yang, W. Li, Z. W. Seh and Y. Cui, *Nano Lett.*, 2013, **13**, 1265–1270.
- 18 Y. Zhang, Z. Bakenov, Y. Zhao, A. Konarov, T. N. L. Doan, M. Malik, T. Paron and P. Chen, *J. Power Sources*, 2012, **208**, 1–8.
- 19 Z. Dong, J. Zhang, X. Zhao, J. Tu, Q. Su and G. Du, *RSC Adv.*, 2013, **3**, 24914–24917.
- 20 Y. Liu, J. Zhang, X. Liu, J. Guo, L. Pan, H. Wang, Q. Su and G. Du, *Mater. Lett.*, 2014, **133**, 193–196.
- 21 F. Wu, J. Chen, R. Chen, S. Wu, L. Li, S. Chen and T. Zhao, *J. Phys. Chem. C*, 2011, **115**, 6057–6063.
- 22 M. Wang, W. Wang, A. Wang, K. Yuan, L. Miao, X. Zhang, Y. Huang, Z. Yu and J. Qiu, *Chem. Commun.*, 2013, **49**, 10263–10265.
- 23 Y. Fu and A. Manthiram, *J. Phys. Chem. C*, 2012, **116**, 8910–8915.
- 24 W. Zhou, Y. Yu, H. Chen, F. J. DiSalvo and H. D. Abruña, *J. Am. Chem. Soc.*, 2013, **135**, 16736–16743.
- 25 L. Xiao, Y. Cao, J. Xiao, B. Schwenzer, M. H. Engelhard, L. V. Saraf, Z. Nie, G. J. Exarhos and J. Liu, *Adv. Mater.*, 2012, **24**, 1176–1181.
- 26 H. P. V. Leeuwen and W. Köster, *Physicochemical Kinetics and Transport at Biointerfaces*, 2004, Wiley.
- 27 H. Zhang, Q. Zhao, S. Zhou, N. Liu, X. Wang, J. Li and F. Wang, *J. Power Sources*, 2011, **196**, 10484–10489.
- 28 S. Zhou, H. Zhang, Q. Zhao, X. Wang, J. Li and F. Wang, *Carbon*, 2013, **52**, 440–450.



An ultrathin sulfur-wrapped PANI nano-composite was well-designed and successfully prepared which displayed superior electrochemical performance.